Time-Domain Calculations of the Polarized Raman Spectra, the Transient Infrared Absorption Anisotropy, and the Extent of Delocalization of the OH Stretching Mode of Liquid Water

Hajime Torii[†]

Department of Chemistry, School of Education, Shizuoka University, 836 Ohya, Shizuoka 422-8529, Japan

Received: April 2, 2006; In Final Form: May 30, 2006

The polarized Raman spectrum and the time dependence of the transient infrared (TRIR) absorption anisotropy are calculated for the OH stretching mode of liquid water (neat liquid H_2O) by using time-domain formulations, which include the effects of both the diagonal frequency modulations (of individual oscillators) induced by the interactions between the dipole derivatives and the intermolecular electric field, and the off-diagonal (intermolecular) vibrational coupling described by the transition dipole coupling (TDC) mechanism. The IR spectrum of neat liquid H_2O and the TRIR anisotropy of a liquid mixture of H_2O/HDO/D_2O are also calculated. It is shown that the calculated features of these optical signals, including the temperature dependence of the polarized Raman and IR spectra, are in reasonable agreement with the experimental results, indicating that the frequency separation between the isotropic and anisotropic components of the polarized Raman spectrum and the rapid decay (∼0.1 ps) of the TRIR anisotropy of the OH stretching mode of neat liquid H_2O are mainly controlled by the resonant intermolecular vibrational coupling described by the TDC mechanism. Comparing with the time evolution of vibrational excitations, it is suggested that the TRIR anisotropy decays in the time needed for the initially localized vibrational excitations to delocalize over a few oscillators. It is also shown that the enhancement of the dipole derivatives by the interactions with surrounding molecules is an important factor in generating the spectral profiles of the OH stretching Raman band. The time-domain behavior of the molecular motions that affect the spectroscopic features is discussed.

1. Introduction

Hydrogen bonding of water molecules is important in the structures, dynamics, and thermodynamics of liquid water and aqueous solutions, as well as in controlling chemical reactions in aqueous solutions and in prompting various functions of biomolecules. It is well-known that the OH stretching mode is sensitive to the hydrogen-bonding condition, and is accessible by various vibrational spectroscopic methods in the time- and frequency domains. As a result, it is highly desirable to correctly understand the relation between the spectroscopic features observed by those methods and the hydrogen-bonding and other properties of liquid water and aqueous solutions.

With the use of ultrashort infrared (IR) pulses, it has been observed that the anisotropy of the transient IR (TRIR) absorption intensity ($v = 1 \rightarrow 2$) of the OH stretching mode of liquid water (neat liquid H_2O) decays vary rapidly with a time constant of ∼70 fs.[1,2] This phenomenon is interpreted as arising from rapid transfer of vibrational excitations among molecules, because the decay becomes much slower upon dilution in D_2O. It has been shown[3,4] that the corresponding phenomenon in the frequency domain is the noncoincidence effect (NCE),[5−24] which is the phenomenon that the isotropic and anisotropic components of the Raman band and the IR band of the same vibrational mode appear at different frequency positions. Strong resonant vibrational coupling between molecules gives rise to rapid transfer of vibrational excitations in the time domain and delocalization of vibrational modes in the frequency domain.

Because of the liquid dynamics, the hydrogen-bonding conditions of individual molecules and the vibrational coupling among molecules are both time-dependent in the liquid phase. As a result, it is necessary to analyze the spectroscopic features on the basis of time-domain formulations. Even for the spectra observed in the frequency domain, effects of liquid dynamics are seen as changes in the band profiles, such as band broadening induced by vibrational dephasing and band narrowing induced by the motional narrowing effect,[25] if the liquid dynamics is sufficiently fast. This problem is especially important in evaluating the extent of delocalization of vibrational excitations in relation to the NCE and the decay of the TRIR anisotropy. Usually, in the frequency-domain picture, the extent of delocalization of vibrational excitations is evaluated by calculating the participation ratio.[26−29] However, in the presence of fast modulations of hydrogen bonding and vibrational coupling, it is considered to be more helpful to evaluate the time evolution of the extent of delocalization of vibrational excitations.[23,24] By calculating this quantity, it is expected that we can interpret the NCE and the decay of the TRIR anisotropy in a more unified way.

In the present study, we calculate the polarized Raman spectrum and the time dependence of the TRIR anisotropy for the OH stretching mode of liquid water (neat liquid H_2O) using time-domain formulations. The IR spectrum of neat liquid H_2O and the TRIR anisotropy of a liquid mixture of H_2O/HDO/D_2O are also calculated. The results are compared with the observed data shown in previous studies,[1,2,30−33] and discussion is made on how the vibrational coupling between molecules affects the spectroscopic features, and how the vibrational frequencies and

[†] Telephone and fax: +81−54−238−4624. E-mail: torii@ed.shizuoka.ac.jp.

10.1021/jp062033s CCC: $33.50
Published on Web 07/12/2006

orientations of individual molecules are modulated by liquid dynamics. We also examine the extent of delocalization of vibrational excitations in relation to the spectroscopic features in the time and frequency domains, and we make comparisons with the cases of some vibrational modes of other liquids.

2. Theoretical Formulation

The time-domain method (called the extended MD/TDC/WFP method) for calculating polarized Raman and IR spectra developed previously[23] is employed in the present study, with an extension to the case of two oscillators in a molecule. The formulation is briefly described as follows. The wave function of the Raman excitation at time t related to the pq element of the polarizability operator α_{pq} (where $p, q = 1, 2, 3$ corresponds to the x, y, and z axes of the system) is expressed as

$$|\psi_{pq}^{(\mathrm{R})}(t, t_0)\rangle = \exp_+\left[-\frac{i}{\hbar}\int_{t_0}^{t} \mathrm{d}\tau\, H^{1\mathrm{Q}}(\tau)\right] |\psi_{pq}^{(\mathrm{R})}(t_0, t_0)\rangle \quad (1)$$

where

$$|\psi_{pq}^{(\mathrm{R})}(t_0, t_0)\rangle = \sum_{m=1}^{N} |m\rangle\langle m \mid \alpha_{pq}(t_0) \mid 0\rangle \quad (2)$$

is the wave function initially made by the Raman excitation at time t_0, expressed by the wave functions of the ground state $|0\rangle$ and the one-quantum ($\upsilon = 1$) excited states $|m\rangle$ on the mth oscillator ($1 \le m \le N$), and the polarizability operator $\alpha_{pq}(t_0)$ evaluated with the molecular orientations at time t_0. This polarizability operator α_{pq} (as well as the dipole operator μ_p that appears below) is an operator for the entire system, so that the product $\alpha_{pq}(t_0)|0\rangle$ (as well as $\mu_p(t_0)|0\rangle$) is expanded by the wave functions of the one-quantum excited states $|m\rangle$ of all the oscillators ($1 \le m \le N$). $H^{1\mathrm{Q}}(\tau)$ is the vibrational Hamiltonian for the one-quantum excited states (defined below). Its diagonal and off-diagonal terms are both dependent on the liquid structures and is therefore time-dependent because of the liquid dynamics, which is calculated by the molecular dynamics (MD) method in the present scheme. N is the number of oscillators participating in the vibrational band in question, so that $|\psi_{pq}^{(\mathrm{R})}(t, t_0)\rangle$ and $H^{1\mathrm{Q}}(\tau)$ are represented by an N-dimensional vector and an $N \times N$ matrix, respectively. Since H_2O has two OH bonds, $N = 2M$ for neat liquid H_2O, where M is the number of molecules in the system. It is assumed as an approximation that the set of $|m\rangle$ ($1 \le m \le N$) forms an orthogonal basis of the space of the $\upsilon = 1$ excited states.

The time-ordered exponential (denoted as $\exp_+$)[34] in eq 1 is evaluated as the product of short-time evolutions assuming that the Hamiltonian is essentially invariant during a very short time period $\Delta\tau$, which is taken as equal to the time step of the MD simulations. We obtain[3,22-24]

$$\begin{aligned}|\psi_{pq}^{(\mathrm{R})}(\tau + \Delta\tau, t_0)\rangle &= \exp\left[-\frac{i}{\hbar}\Delta\tau\, H^{1\mathrm{Q}}(\tau)\right]|\psi_{pq}^{(\mathrm{R})}(\tau, t_0)\rangle \\ &= \sum_{\xi=1}^{N} |\xi'_\tau\rangle \exp[-i\omega_\xi(\tau)\,\Delta\tau\,]\langle\xi_\tau|\psi_{pq}^{(\mathrm{R})}(\tau, t_0)\rangle \end{aligned} \quad (3)$$

where $\omega_\xi(\tau)$ is the vibrational frequency for the eigenstate $|\xi_\tau\rangle$ (numbered by ξ) of $H^{1\mathrm{Q}}(\tau)$, and $|\xi'_\tau\rangle$ is the wave function with the same amplitudes of molecular vibrations as $|\xi_\tau\rangle$ but with the molecular orientations evaluated at time $\tau + \Delta\tau$. This equation describes a finite-difference approximation that becomes exact as $\Delta\tau \to 0$, in the same way as the equations for the molecular translations and rotations (of MD simulations).

Assuming $\hbar\omega \gg kT$, the Raman spectrum $I_{pq}^{(\mathrm{R})}(\omega)$ is expressed as

$$I_{pq}^{(\mathrm{R})}(\omega) = \mathrm{Re}\int_0^\infty dt\, \exp(i\omega\, t)\left\langle\langle 0\,|\alpha_{pq}(t)\,|\psi_{pq}^{(\mathrm{R})}(t,0)\rangle\right\rangle \quad (4)$$

where the large bracket stands for statistical average, assuming that the effect of vibrational population relaxation is negligible. The isotropic and anisotropic components of the Raman spectrum are obtained from appropriate combinations of $I_{pq}^{(\mathrm{R})}(\omega)$ with $p, q = 1, 2, 3$. In the same way, the IR spectrum $I_p^{(\mathrm{IR})}(\omega)$ is expressed as

$$I_p^{(\mathrm{IR})}(\omega) = \mathrm{Re}\int_0^\infty \mathrm{d}t\, \exp(i\omega\, t)\left\langle\langle 0 \mid \mu_p(t)\,|\psi_p^{(\mathrm{IR})}(t,0)\rangle\right\rangle \quad (5)$$

where $|\psi_p^{(\mathrm{IR})}(t, t_0)\rangle$ is the wave function of the IR excitation at time t, given as

$$|\psi_p^{(\mathrm{IR})}(t, t_0)\rangle = \exp_+\left[-\frac{i}{\hbar}\int_{t_0}^{t} \mathrm{d}\tau\, H^{1\mathrm{Q}}(\tau)\right]|\psi_p^{(\mathrm{IR})}(t_0, t_0)\rangle \quad (6)$$

with

$$|\psi_p^{(\mathrm{IR})}(t_0, t_0)\rangle = \sum_{m=1}^{N} |m\rangle\langle m|\mu_p(t_0)|0\rangle \quad (7)$$

and $\mu_p(t)$ is the dipole operator evaluated with the molecular orientations at time t. The time-ordered exponential in eq 6 is evaluated in the same way as shown in eq 3 for $|\psi_{pq}^{(\mathrm{R})}(t, t_0)\rangle$.

The TRIR absorption intensity at delay time t from the pump pulse is expressed as[4]

$$D_{qp}(t) = \left\langle \sum_{\lambda=1}^{N} |\langle\lambda_t^{\mathrm{ov}}|U_q(t)\,|\psi_p^{(\mathrm{IR})}(t, 0)\rangle|^2 \right\rangle \quad (8)$$

In eq 8, $|\lambda_t^{\mathrm{ov}}\rangle$ is an eigenstate (numbered by λ) in the overtone band[35] at time t, and $U_q(t)$ is the transition operator between the one-quantum and two-quantum excited states. Within the harmonic approximation for $U_q(t)$, and assuming that the overtone band is spectrally separated from the combination band, we have[4]

$$D_{qp}(t) \cong \left\langle \sum_{m=1}^{N} 2\,|\langle m|\mu_q(t)|0\rangle|^2|\langle m|\psi_p^{(\mathrm{IR})}(t,0)\rangle|^2 \right\rangle \quad (9)$$

The TRIR anisotropy is then given as

$$A(t) = \frac{D_{//}(t) - D_{\perp}(t)}{D_{//}(t) + 2D_{\perp}(t)} \quad (10)$$

with

$$D_{||}(t) = D_{pp}(t) \quad (11)$$

$$D_{\perp}(t) = \frac{1}{2}\sum_{q(\neq p)} D_{qp}(t) \quad (12)$$

The vibrational population relaxation (to the overtone of the HOH bending mode, etc.) is not considered to affect the TRIR anisotropy $A(t)$, because it is expected to reduce both the

denominator and the numerator of eq 10, keeping the value of the ratio.

The vibrational Hamiltonian H^{1Q} is constructed as follows, from the liquid structures and dynamics obtained in the MD simulations. The modulations in the diagonal terms of H^{1Q} (the shift from $\hbar\sqrt{k_m}$) are assumed to be controlled by the electric field from the surrounding molecules,[23,24,36−44] and are expressed as[23,24,45−47]

$$\Delta H^{1Q}_{mm} = \frac{\hbar}{2\sqrt{k_m}}\left(\frac{f_m}{k_m}\frac{\partial \boldsymbol{\mu}_m}{\partial q_m} - \frac{\partial^2 \boldsymbol{\mu}_m}{\partial q_m^2}\right)\boldsymbol{E}_m \qquad (13)$$

where k_m and f_m are the diagonal quadratic and cubic force constants for the vibration of the mth oscillator (q_m), and $\boldsymbol{E}_m$ is the electric field operating on the mth oscillator from the surrounding molecules. The off-diagonal terms of H^{1Q} are classified into two types. The coupling between the oscillators of different molecules[48−52] is assumed to be determined by the transition dipole coupling (TDC) mechanism,[20−24,53,54] expressed as

$$H^{1Q}_{mn} = -\frac{\hbar}{2(k_m k_n)^{1/4}}\frac{\partial \boldsymbol{\mu}_m}{\partial q_m}\boldsymbol{T}_{mn}\frac{\partial \boldsymbol{\mu}_n}{\partial q_n} \qquad [(m, n) \in \text{different molecules}] \quad (14)$$

where $\boldsymbol{T}_{mn}$ is the dipole interaction tensor between the mth and nth oscillators, which is given as

$$\boldsymbol{T}_{mn} = \frac{3\boldsymbol{r}_{mn}\boldsymbol{r}_{mn} - r_{mn}{}^2\boldsymbol{I}}{r_{mn}{}^5} \qquad (15)$$

where $\boldsymbol{r}_{mn} = \boldsymbol{r}_m - \boldsymbol{r}_n$ is the distance vector (of length r_{mn}) between the two oscillators, and $\boldsymbol{I}$ is a 3×3 unit tensor. Equation 14 applies to hydrogen-bonded as well as distant pairs of molecules, meaning that the present method deals with the vibrational interactions between all the pairs of molecules in a unified way, rather than assuming a special interaction mechanism for hydrogen-bonded pairs.[49,50] As for the intramolecular coupling terms k'_{mn} [$(m, n) \in$ identical molecule], comparison of the observed and calculated dispersion of the depolarization ratio (described below in section 4A) suggests that k'_{mn} of H_2O in liquid water is much smaller than that of an isolated H_2O molecule. Therefore, in the present study, k'_{mn} is assumed to be zero for all the molecules unless otherwise stated explicitly.

Considering that the IR intensity (proportional to the square of the dipole derivative) of the OH stretching mode is very sensitive to the hydrogen-bonding condition, the dipole derivatives appearing in eqs 13 and 14 are assumed to be enhanced by the electric field from the surrounding molecules.[55−57] The enhancement factor $\zeta \equiv \partial(\partial\mu/\partial q)/\partial E$ is treated as an adjustable parameter, as described below in section 3.

3. Computational Procedure

The parameters of molecular properties needed for constructing the vibrational Hamiltonian were determined as follows. The value of k_m was determined from the average of the observed frequencies of the symmetric and antisymmetric OH stretching modes of H_2O in the gas phase (3656.65 and 3755.79 cm^{-1})[58] as $k_m = 28.5163 \times 10^{-5}\ E_h\ a_0^{-2}\ m_e^{-1}$ (=8.0931 mdyn $Å^{-1}$ amu^{-1}). The ratio f_m/k_m was calculated as $f_m/k_m = -9.370 \times 10^{-2}\ a_0^{-1}\ m_e^{-1/2}$ by the ab initio molecular orbital (MO) method at the MP3/6-31+G(2df,p) level (by using Gaussian 03[59]) for the stretching of the hydrogen-bonded OH bonds in the cyclic H_2O hexamer, $(H_2O)_6$, with a chair-form hydrogen-bonded backbone.[60] To obtain a better agreement between the observed[30,31,33] and calculated vibrational frequency positions, however, we reduced the magnitude to 85% of this value ($f_m/k_m = -7.965 \times 10^{-2}\ a_0^{-1}\ m_e^{-1/2}$). In fact, the value of f_m/k_m calculated for an isolated H_2O molecule ($= -8.536 \times 10^{-2}\ a_0^{-1}\ m_e^{-1/2}$) was closer to this reduced value. The dipole derivative $\partial\boldsymbol{\mu}_m/\partial q_m$ was determined also by referring to the result of the ab initio MO calculation for the cyclic $(H_2O)_6$. According to this calculation, $\partial\boldsymbol{\mu}_m/\partial q_m$ of the stretching of the hydrogen-bonded OH (of magnitude equal to $2.0004 \times 10^{-2}\ e\ m_e^{-1/2}$) was almost parallel to the OH bond, and the projection of $\partial\boldsymbol{\mu}_m/\partial q_m$ onto the OH bond was $0.6212 \times 10^{-2}\ e\ m_e^{-1/2}$ for the stretching of the free OH. As a result, we assumed as an approximation that $\partial\boldsymbol{\mu}_m/\partial q_m$ is parallel to the OH bond, and $|(\partial\boldsymbol{\mu}_m/\partial q_m)_0| = 0.6 \times 10^{-2}\ e\ m_e^{-1/2}$ as the value at $\boldsymbol{E}_m = 0$. The enhancement factor ζ was varied in the range of $0.35-0.26\ e^2\ m_e^{-1/2}\ a_0\ E_h^{-1}$ (estimated from $|(\partial\boldsymbol{\mu}_m/\partial q_m)| \cong 2 \times 10^{-2}\ e\ m_e^{-1/2}$ and the magnitude of the electric field in liquid water) as an adjustable parameter. The dipole second derivative $\partial^2\boldsymbol{\mu}_m/\partial q_m{}^2$ was neglected in the present study, since its effect seems to be smaller than that of ζ. In constructing the vibrational Hamiltonian, the interaction point of the dipole derivative was assumed to be located at the site of the hydrogen atom, as suggested in the previous studies.[40,56,57] The Raman tensor ($\equiv\langle m|\alpha_{pq}|0\rangle$ in eq 2) needed to calculate the Raman spectrum was assumed to be axially symmetric with respect to the OH bond, with the ratio $\alpha_{\parallel}:\alpha_{\perp} = 5.7:1$. In fact, only the overall intensity ratio between the isotropic and anisotropic components but not the band profile of each component is affected by varying this ratio.

For comparison, we also calculated the polarized Raman and IR spectra with $|(\partial\boldsymbol{\mu}_m/\partial q_m)_0| = 2.0 \times 10^{-2}\ e\ m_e^{-1/2}$ and $\zeta = 0$ to clearly see the effect of ζ on the band profiles.

The MD simulations for calculating the polarized Raman and IR spectra and the time dependence of the TRIR anisotropy were carried out for the liquid system of 128 molecules in a cubic cell by using the TIP3P model potential.[61] The temperature was set at 263, 283, 303, 323, 343, and 363 K in calculating polarized Raman and IR spectra to make comparison between the experiment[31,33] and calculation with regard to the temperature dependence of the band profiles, and at 298 K in calculating the time dependence of the TRIR anisotropy. The time dependence of the TRIR anisotropy was also calculated for a liquid mixture of $H_2O/HDO/D_2O$ with 3 H_2O, 33 HDO, and 92 D_2O (H:D = 1:5.56). The volume of the cubic cell was fixed by referring to the experimental density of liquid water.[62] The time step $\Delta\tau$ was set to 1 fs. In calculating polarized Raman and IR spectra, the time evolution of $|\psi^{(R)}_{pq}(t,t_0)\rangle$ and $|\psi^{(IR)}_{p}(t,t_0)\rangle$ was calculated for ~16.4 ps (16384 time steps) to obtain a frequency resolution of ~2 cm^{-1}, and the spectra were averaged over 2250 samples to get good statistics. The calculated TRIR anisotropy was averaged over 1350 samples. Taking into account the diffusion constant ($(1.9-2.3) \times 10^{-5}$ cm^2 s^{-1}) of liquid water,[63] it is considered that the full length of the simulations for the TRIR anisotropy (~26.5 ns) is long enough for sufficient mixing of the three isotopic species (H_2O, HDO, and D_2O).

The calculations were carried out on Hewlett-Packard zx6000 and other workstations with our original programs. Parts of the calculations were also carried out on TX-7 computers at the Research Center for Computational Science of the National Institutes of Natural Sciences at Okazaki. The computation time needed to calculate polarized Raman and IR spectra (at one specified temperature with one set of molecular parameters, as

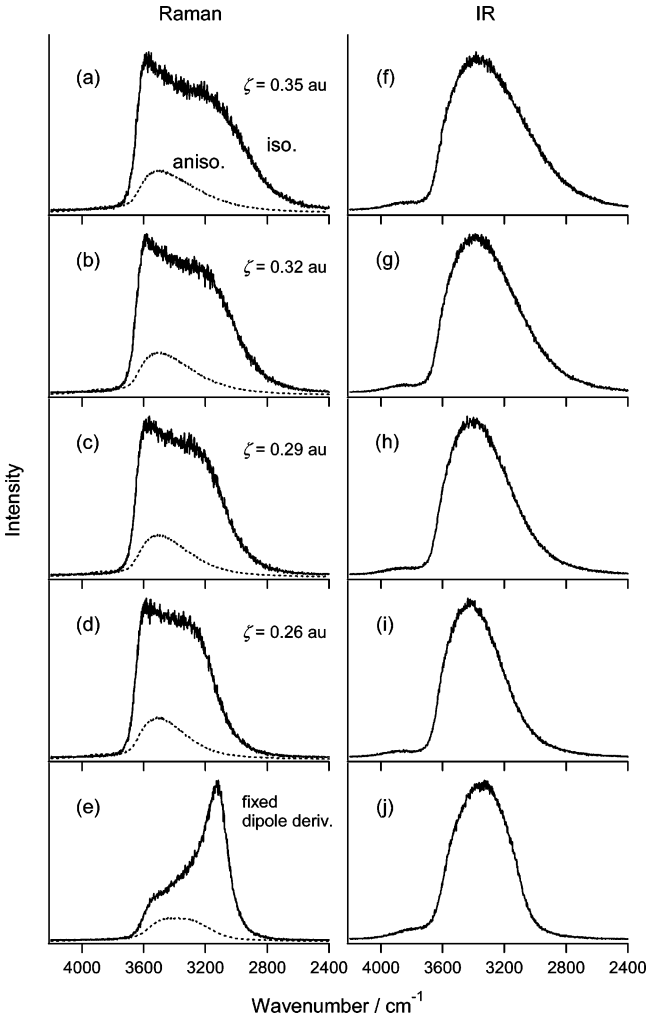

Figure 1. (a−e) Polarized Raman spectra of the OH stretching mode of neat liquid H_2O at 303 K calculated with $|(\partial\boldsymbol{\mu}_m/\partial q_m)_0| = 0.6 \times 10^{-2}\ e\ m_e^{-1/2}$ and (a) $\zeta = 0.35$, (b) 0.32, (c) 0.29, and (d) 0.26 $e^2\ m_e^{-1/2}\ a_0\ E_h^{-1}$ (atomic unit), and (e) with a fixed dipole derivative ($\zeta = 0$) of $|(\partial\boldsymbol{\mu}_m/\partial q_m)_0| = 2.0 \times 10^{-2}\ e\ m_e^{-1/2}$. The value of k'_{mn} is set to be zero. Solid line: isotropic component, dotted line: anisotropic component. (f−j) IR spectra calculated with the same sets of parameters.

averages over 2250 samples) was equivalent to ∼760 h of a single zx6000 (Itanium-2, 1.5 GHz/6MB cache) CPU time.

4. Results and Discussion

A. Polarized Raman and IR Spectra. The polarized Raman and IR spectra calculated for the OH stretching mode of liquid water (neat liquid H_2O) with $|(\partial\boldsymbol{\mu}_m/\partial q_m)_0| = 0.6 \times 10^{-2}\ e\ m_e^{-1/2}$ and four different values of ζ in the range of 0.35−0.26 $e^2\ m_e^{-1/2}\ a_0\ E_h^{-1}$ (atomic unit) at 303 K are shown in Figure 1, parts a−d and f−i. The spectra calculated with $|(\partial\boldsymbol{\mu}_m/\partial q_m)_0| = 2.0 \times 10^{-2}\ e\ m_e^{-1/2}$ and $\zeta = 0$ are also shown for comparison (Figure 1e and j). It is seen that, irrespective of the value of ζ in the range of 0.35−0.26 $e^2\ m_e^{-1/2}\ a_0\ E_h^{-1}$, two bands of comparable intensities appear in the isotropic Raman spectrum, and the higher-frequency one is located close to the peak of the anisotropic Raman spectrum, in reasonable agreement with the observed spectral features.[30,31] These bands cannot be regarded as arising from the symmetric and antisymmetric OH stretching modes of H_2O that arise from the intramolecular vibrational coupling k'_{mn}, because the antisymmetric OH stretching mode is not totally symmetric and, hence, would have vanishing isotropic Raman intensity. It is more appropriate to consider the spectral features in the OH stretching region as a whole. From this viewpoint, the frequency separation between the first moments of the isotropic and anisotropic Raman spectra shown in Figure 1a−e is interpreted as the NCE, with both bands in the isotropic Raman spectrum being related to the same band at ∼3500 cm^{-1} in the anisotropic Raman spectrum. It is also seen that, if we assume $\zeta = 0$, the lower-frequency band becomes much stronger in the isotropic Raman spectrum. This result suggests that the enhancement of the dipole derivatives by the interactions with surrounding molecules is an important factor in generating the spectral profiles of the OH stretching Raman bands, in agreement with the results obtained in the previous studies.[56,57] By contrast, the IR band profile shown in Figure 1f-j is rather insensitive to this enhancement factor, with the peak located at ∼3400 cm^{-1} in agreement with the experimental result.[33]

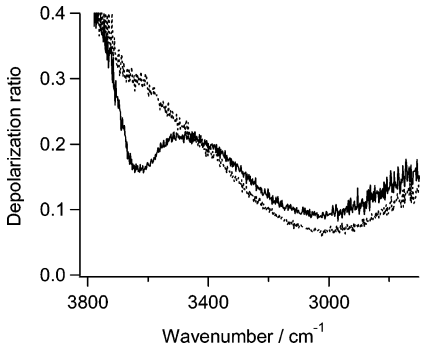

Figure 2. Frequency dependence of the depolarization ratio in the OH stretching Raman band of neat liquid H_2O at 303 K calculated with $|(\partial\boldsymbol{\mu}_m/\partial q_m)_0| = 0.6 \times 10^{-2}\ e\ m_e^{-1/2}$ and $\zeta = 0.32\ e^2\ m_e^{-1/2}\ a_0\ E_h^{-1}$. Solid line: the case of $k'_{mn} = 0$, dotted line: the case of $k'_{mn} = -0.7628 \times 10^{-5}\ E_h\ a_0^{-2}\ m_e^{-1}$.

The existence of the NCE means that dispersion is present in the depolarization ratio (denoted as ρ hereafter). The spectrum of ρ calculated with $|(\partial\boldsymbol{\mu}_m/\partial q_m)_0| = 0.6 \times 10^{-2}\ e\ m_e^{-1/2}$ and $\zeta = 0.32\ e^2\ m_e^{-1/2}\ a_0\ E_h^{-1}$ is shown with a solid line in Figure 2. (Similar spectra are calculated with the other values of ζ in the range $0.35-0.26\ e^2\ m_e^{-1/2}\ a_0\ E_h^{-1}$.) It is seen that a maximum ($\rho \cong 0.21$) and a minimum ($\rho \cong 0.09$) appear at ∼3500 and ∼3050 cm^{-1}, respectively, in reasonable agreement with the experimental result [$(\tilde{\nu}/cm^{-1},\ \rho) \cong$ (3585, 0.25) and (3130, 0.05)].[32] The calculated feature in the frequency region above 3600 cm^{-1} arises from the high-frequency tail of the band, and will not be discussed further.

If we set k'_{mn} [$(m, n) \in$ identical molecule] as $-0.7628 \times 10^{-5}\ E_h\ a_0^{-2}\ m_e^{-1}$ (= −0.2165 mdyn $Å^{-1}$ amu^{-1}, the value estimated from the observed frequencies of the symmetric and antisymmetric OH stretching modes of H_2O in the gas phase[58]), the maximum in the spectrum of ρ at ∼3500 cm^{-1} disappears as shown with a dotted line in Figure 2. This result suggests that the intramolecular coupling of the OH stretching mode of H_2O in liquid water is much smaller than that of an isolated H_2O molecule. A similar conclusion has been obtained in some previous studies.[64−66]

The temperature dependence of the polarized Raman and IR band profiles in the range of 263−363 K calculated with $|(\partial\boldsymbol{\mu}_m/\partial q_m)_0| = 0.6 \times 10^{-2}\ e\ m_e^{-1/2}$ and $\zeta = 0.32\ e^2\ m_e^{-1/2}\ a_0\ E_h^{-1}$ is shown in Figure 3. It is seen that, as the temperature decreases, the lower-frequency band is enhanced and the higher-frequency band is reduced in the isotropic Raman spectrum (Figure 3a). This result is also in reasonable agreement with the experimental result,[31] although the height of the lower-frequency band is a little too low at 263 and 283 K. A similar but

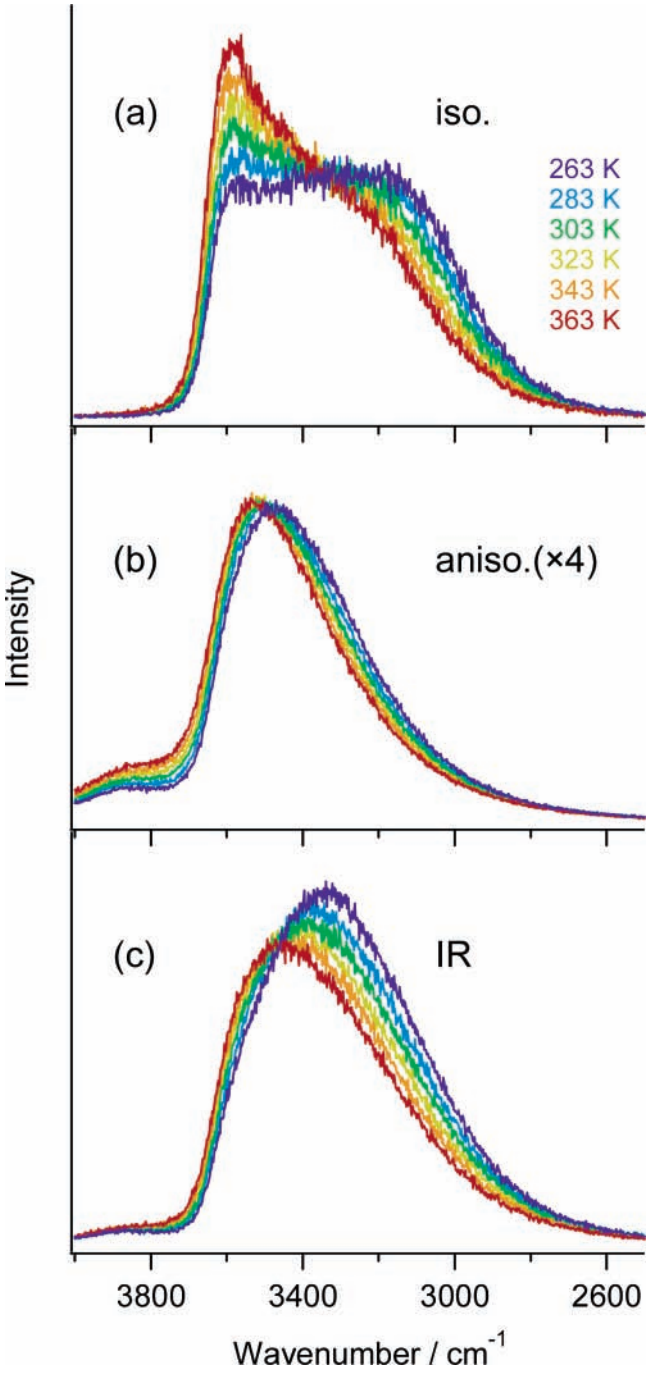

Figure 3. (a) Isotropic Raman, (b) anisotropic Raman, and (c) IR spectra of the OH stretching mode of neat liquid H_2O at 263, 283, 303, 323, 343, and 363 K calculated with $|(\partial \boldsymbol{\mu}_m/\partial q_m)_0| = 0.6 \times 10^{-2}\ e\ m_e^{-1/2}$, $\zeta = 0.32\ e^2\ m_e^{-1/2}\ a_0\ E_h^{-1}$, and $k'_{mn} = 0$. The intensities of the anisotropic Raman spectra are magnified by the factor of 4 as compared with the isotropic Raman spectra.

less significant change is obtained for the IR band (Figure 3c), in agreement with the observed temperature dependence (at 264−320 K).[33] These changes in the band profiles are considered to be related to the variation in the hydrogen-bonding conditions. The enhancement of the total intensity of the IR spectrum that occurs upon decreasing temperature arises from a combined effect of the strengthening of hydrogen bonds and the enhancement factor ζ. The dependence of these features on the model potential (such as the TIP*n*P models[67]) will be studied in a future study.

B. Distribution of Intermolecular Vibrational Coupling Constants. To see the distribution of the intermolecular vibrational coupling constants (H^{1Q}_{mn} defined in eq 14) in detail, the coupling constants of all the oscillator pairs belonging to different molecules, the number of which is equal to $2M(M-1)$, are arranged in the sequence of their sign-reverted values or absolute values, and are plotted against their sequential numbers divided by M, regarded as the number of neighboring oscillators (denoted as N_B hereafter). Plotting sign-reverted values is essentially equivalent to taking only negative coupling constants. The result (calculated with $|(\partial \boldsymbol{\mu}_m/\partial q_m)_0| = 0.6 \times 10^{-2}\ e\ m_e^{-1/2}$ and $\zeta = 0.32\ e^2\ m_e^{-1/2}\ a_0\ E_h^{-1}$) is shown as a semilog plot in Figure 4a and a log−log plot in Figure 4b. It is seen that almost all of the large coupling constants ($\geq 3 \times 10^{-6}\ E_h\ a_0^{-2}\ m_e^{-1}$) are negative, as expected from the arrangement of the hydrogen-bonded OH bonds (...H−O···H−O...), and the magnitude decreases as a power of N_B in the region of $N_B > 1$. When we take only the negative coupling constants, the magnitude decreases as $N_B^{-1.29}$. Supposing that $N_B \sim r^3$, where r is the intermolecular distance, this behavior is equivalent to $r^{-3.88}$, faster than the r^{-3} dependence arising from the denominator of H^{1Q}_{mn}. Even $|H^{1Q}_{mn}|$ decreases faster than r^{-3}, as $N_B^{-1.07}$ (equivalent to $r^{-3.21}$). This faster dependence of the magnitude of the coupling constant is related to the orientational factor

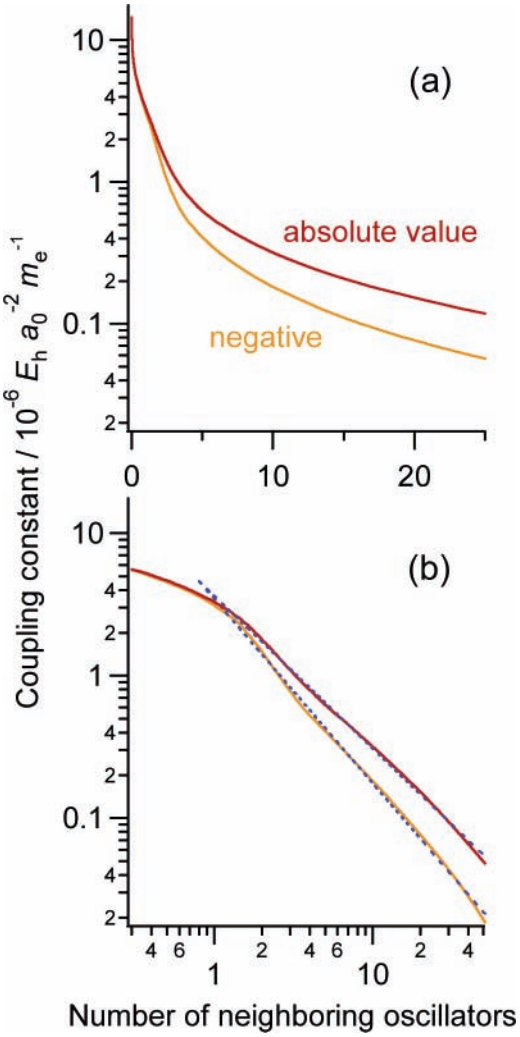

Figure 4. Distribution of the intermolecular vibrational coupling constants ($-H^{1Q}_{mn}$ and $|H^{1Q}_{mn}|$ defined in eq 14) plotted against the number of neighboring oscillators (N_B, defined in the text), calculated for the OH stretching mode of neat liquid H_2O at 303 K with $|(\partial \boldsymbol{\mu}_m/\partial q_m)_0| = 0.6 \times 10^{-2}\ e\ m_e^{-1/2}$ and $\zeta = 0.32\ e^2\ m_e^{-1/2}\ a_0\ E_h^{-1}$. (a) A semilog plot, and (b) a log−log plot. The blue dotted lines in part b show the dependence of $\sim N_B^{-1.29}$ and $\sim N_B^{-1.07}$.

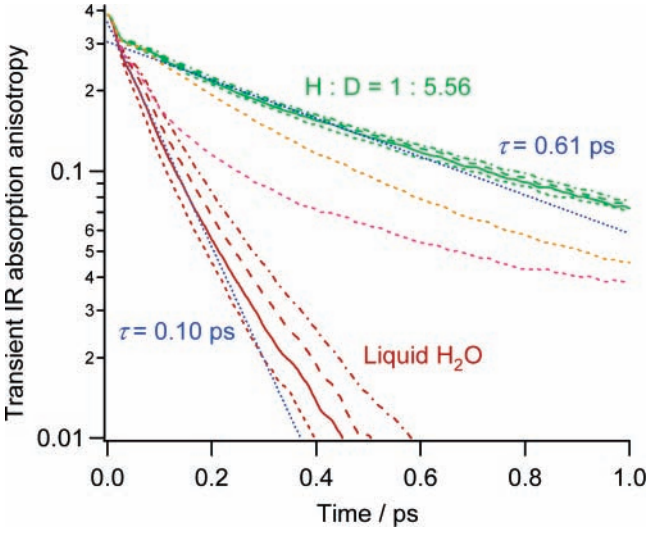

Figure 5. Red and green lines: the time dependence of the TRIR anisotropy calculated for the OH stretching mode of neat liquid H_2O (red lines) and a liquid mixture of H_2O/HDO/D_2O with H:D = 1:5.56 (green lines) at 298 K calculated with $|(\partial\boldsymbol{\mu}_m/\partial q_m)_0| = 0.6 \times 10^{-2}\ e\ m_e^{-1/2}$ and $k'_{mn} = 0$. The value of ζ is set as $\zeta = 0.35$, 0.32, 0.29, and $0.26\ e^2\ m_e^{-1/2}\ a_0\ E_h^{-1}$ (dotted, solid, broken, and dot−dashed lines, respectively). Blue dotted lines: the decay curves with a time constant of $\tau = 0.10$ and 0.61 ps. Pink and orange dotted lines: the time dependence of the TRIR anisotropy calculated for the OH stretching mode of neat liquid H_2O at 298 K calculated with $|(\partial\boldsymbol{\mu}_m/\partial q_m)_0| = 0.6 \times 10^{-2}\ e\ m_e^{-1/2}$, $\zeta = 0.32\ e^2\ m_e^{-1/2}\ a_0\ E_h^{-1}$, and $k'_{mn} = -0.7628 \times 10^{-5}$ (pink) and $-0.3814 \times 10^{-5}\ E_h\ a_0^{-2}\ m_e^{-1}$ (orange), but with all the intermolecular vibrational couplings being switched off.

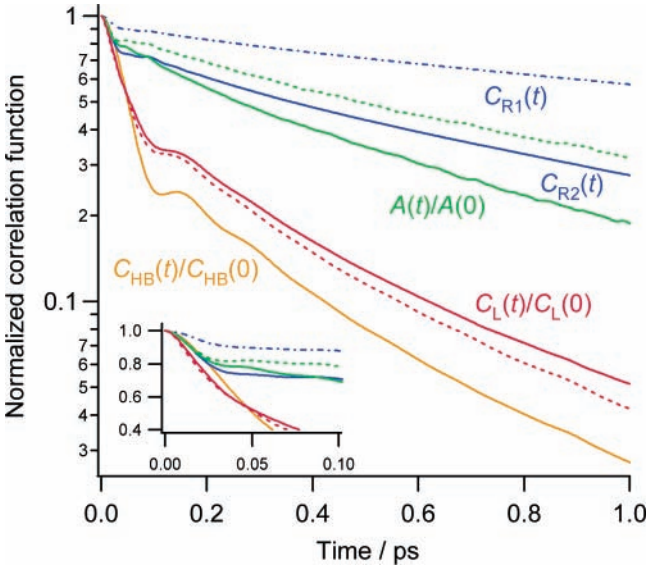

Figure 6. Blue lines: the time correlation functions $C_{R1}(t)$ and $C_{R2}(t)$ (dot−dashed and solid lines, respectively) of the $\boldsymbol{n}_{OH}$ vectors calculated for a liquid mixture of H_2O/HDO/D_2O (H:D = 1:5.56) at 298 K. Orange line: the normalized time correlation function $C_{HB}(t)/C_{HB}(0)$ of the hydrogen-bond lengths as defined by eq 21 calculated for H_2O/HDO/D_2O. Red lines: the normalized time correlation function $C_L(t)/C_L(0)$ of the modulations of the vibrational frequencies calculated for the OH stretching mode of H_2O/HDO/D_2O (solid line) and neat liquid H_2O (dotted line) with $|(\partial\boldsymbol{\mu}_m/\partial q_m)_0| = 0.6 \times 10^{-2}\ e\ m_e^{-1/2}$ and $\zeta = 0.32\ e^2\ m_e^{-1/2}\ a_0\ E_h^{-1}$. Green solid line: the normalized time dependence of the TRIR anisotropy calculated for the OH stretching mode of H_2O/HDO/D_2O with $|(\partial\boldsymbol{\mu}_m/\partial q_m)_0| = 0.6 \times 10^{-2}\ e\ m_e^{-1/2}$, $\zeta = 0.32\ e^2\ m_e^{-1/2}\ a_0\ E_h^{-1}$, and $k'_{mn} = 0$ (denoted as $[A(t)/A(0)]_{vc\neq0,\zeta=0.32}$ in the text). Green dotted line: the same quantity calculated in the case where all the intermolecular and intramolecular vibrational couplings are switched off but the modulations of the dipole derivatives are fully retained (denoted as $[A(t)/A(0)]_{vc=0,\zeta=0.32}$ in the text).

(the numerator) of H_{mn}^{1Q} in eq 14. It is also true, however, that this dependence is not too far from r^{-3}, in contrast to the case of strictly isotropic orientation (isotropic even on the molecular scale).[68] This property is not peculiar to liquid water or hydrogen-bonding liquids. For example, in the case of the C=O stretching mode of liquid acetone,[23] which is a nonprotic polar liquid, the dependence of $-H_{mn}^{1Q}$ and $|H_{mn}^{1Q}|$ against N_B is calculated as $N_B^{-1.31}$ and $N_B^{-1.03}$, respectively.

C. Time Dependence of the TRIR Anisotropy and Related Correlation Functions. The time dependence of the TRIR anisotropy $A(t)$ calculated for the OH stretching mode of neat liquid H_2O and a liquid mixture of H_2O/HDO/D_2O (H:D = 1:5.56) with $|(\partial\boldsymbol{\mu}_m/\partial q_m)_0| = 0.6 \times 10^{-2}\ e\ m_e^{-1/2}$ and four different values of ζ in the range of $0.35-0.26\ e^2\ m_e^{-1/2}\ a_0\ E_h^{-1}$ at 298 K are shown with red and green lines, respectively, in Figure 5. It is clearly seen that the TRIR anisotropy decays very rapidly in neat liquid H_2O but the decay rate becomes much slower when it is diluted in D_2O. The time constant of the decay (in the case of $\zeta = 0.32\ e^2\ m_e^{-1/2}\ a_0\ E_h^{-1}$, shown in solid lines) is calculated as $\tau = 0.10$ ps for neat liquid H_2O from the fit in the time range of $t = 0.00-0.20$ ps, and as $\tau = 0.61$ ps for the liquid mixture of H_2O/HDO/D_2O from the fit in the time range of $t = 0.05-0.60$ ps, in reasonable agreement with the observed value ($\tau = 0.07$ and 0.70 ps, the latter for H:D = 1:6).[2]

When we neglect all the intermolecular vibrational coupling and increase the magnitude of the intramolecular vibrational coupling k'_{mn} instead, we obtain the decay of the TRIR anisotropy for neat liquid H_2O as shown with pink and orange dotted lines (for $k'_{mn} = -0.7628 \times 10^{-5}$ and $-0.3814 \times 10^{-5}\ E_h\ a_0^{-2}\ m_e^{-1}$, respectively) in Figure 5. It is seen that the TRIR anisotropy remains larger than 0.04 even at a time close to 1 ps, in contrast to the experimental result.[1,2] This result confirms that the rapid decay of the TRIR anisotropy observed for the OH stretching mode of neat liquid H_2O mainly arises from the resonant intermolecular vibrational coupling, and the TDC mechanism described by eq 14 reasonably explains this vibrational coupling. It also suggests that the decay rate is not much affected by intramolecular vibrational coupling as far as its magnitude is less than $\sim 0.4 \times 10^{-5}\ E_h\ a_0^{-2}\ m_e^{-1}$.

It is noticed from the plot in Figure 5 that, in the first 25 fs, the TRIR anisotropy decays rapidly even in the case of the liquid mixture of H_2O/HDO/D_2O, from 0.4 at $t = 0$ fs to $\sim$0.33 at $t = 25$ fs. This initial rapid decay has also been observed experimentally.[69−71] To examine the reason for this behavior, the time correlation functions of the $\boldsymbol{n}_{OH}$ ($\equiv \boldsymbol{r}_{OH}/|\boldsymbol{r}_{OH}|$, $\boldsymbol{r}_{OH} = \boldsymbol{r}_H - \boldsymbol{r}_O$) vectors defined as

$$C_{R1}(t) = \langle \boldsymbol{n}_{OH}(t)\cdot\boldsymbol{n}_{OH}(0)\rangle \tag{16}$$

$$C_{R2}(t) = \frac{1}{2}\langle 3[\boldsymbol{n}_{OH}(t)\cdot\boldsymbol{n}_{OH}(0)]^2 - 1\rangle \tag{17}$$

are calculated. The result is shown with blue lines in Figure 6. The normalized TRIR anisotropy $A(t)/A(0)$ is also plotted with a green solid line for comparison. It is seen that $C_{R2}(t)$ decays rapidly to $\sim$0.77 in the first 30 fs,[69,72] in a manner similar to that seen for $A(t)/A(0)$. A similar (but smaller) decay is also seen for $C_{R1}(t)$. The time constant of this decay corresponds to the librations of water molecules, observed in the low-frequency Raman spectrum in the 450−800 cm^{-1} region.[73] This result suggests that the initial rapid decay of $A(t)$ calculated for the liquid mixture of H_2O/HDO/D_2O mainly arises from the librations of water molecules.

In fact, $C_{R2}(t)$ is equivalent to $A(t)/A(0)$ in the case where all the intermolecular and intramolecular vibrational couplings and the modulations of the dipole derivatives (induced by ζ and $\boldsymbol{E}$) are switched off, denoted as $[A(t)/A(0)]_{vc=0,\zeta=0}$. Then, a problem arises as to what is the origin of the difference between $C_{R2}(t)$ and $A(t)/A(0)$ of $H_2O/HDO/D_2O$ shown in Figure 6. (Hereafter, the latter is denoted as $[A(t)/A(0)]_{vc\neq 0,\zeta=0.32}$ for clarity.) To examine this problem, $A(t)/A(0)$ is calculated for the case where all the intermolecular and intramolecular vibrational couplings are switched off but the modulations of the dipole derivatives are fully retained ($\zeta = 0.32\ e^2\ m_e^{-1/2}\ a_0\ E_h^{-1}$), denoted as $[A(t)/A(0)]_{vc=0,\zeta=0.32}$. The result is shown with a green dotted line in Figure 6. It is seen that, in the same way as $[A(t)/A(0)]_{vc\neq 0,\zeta=0.32}$, the initial decay of $[A(t)/A(0)]_{vc=0,\zeta=0.32}$ in the first 50 fs is slightly shallower than that of $C_{R2}(t)$, suggesting that this difference arises from the modulations of the dipole derivatives. In contrast, the slightly faster decay of $[A(t)/A(0)]_{vc\neq 0,\zeta=0.32}$ in the region of $t \geq 0.2$ ps is considered to be due to the weak intermolecular vibrational coupling among the OH oscillators present even in the liquid mixture of $H_2O/HDO/D_2O$.

In relation to the behavior of $C_{R2}(t)$, the time correlation function of the modulations of the vibrational frequencies has also been discussed.[38,69,70] It is defined as

$$C_L(t) = \left\langle \frac{1}{N}\sum_{m=1}^{N} \delta\tilde{\nu}_m^{(L)}(t)\delta\tilde{\nu}_m^{(L)}(0) \right\rangle \tag{18}$$

where

$$\delta\tilde{\nu}_m^{(L)}(t) = \tilde{\nu}_m^{(L)}(t) - \left\langle \frac{1}{N}\sum_{m=1}^{N} \tilde{\nu}_m^{(L)} \right\rangle \tag{19}$$

and $\tilde{\nu}_m^{(L)}(t)$ is the (uncoupled) vibrational frequency of the mth oscillator [equal to the mth diagonal element of the vibrational Hamiltonian, $H_{mm}^{1Q}(t)$] at time t. The result obtained in the present study for $H_2O/HDO/D_2O$ with $|(\partial\boldsymbol{\mu}_m/\partial q_m)_0| = 0.6 \times 10^{-2}\ e\ m_e^{-1/2}$ and $\zeta = 0.32\ e^2\ m_e^{-1/2}\ a_0\ E_h^{-1}$ is shown with a red solid line in Figure 6. It is seen that $C_L(t)/C_L(0)$ decays rapidly to ~0.35 in the first 100 fs, exhibiting a small bump in the 100−150 fs region, and decays more slowly at later times. Similar behavior has been obtained in previous studies.[38,74] Experimentally, $C_L(t)$ is obtained from the measurement of the photon echo peak shift.[38,75,76] The calculated behavior described above is in reasonable agreement with the experimental result, suggesting the validity of the mechanism of the frequency modulations described by eq 13. The similarity of the behavior of $C_L(t)/C_L(0)$ between neat liquid H_2O (red dotted line in Figure 6) and $H_2O/HDO/D_2O$ indicates that measurements on $H_2O/HDO/D_2O$ are appropriate for obtaining information on the frequency modulations of the OH stretching mode in neat liquid H_2O.

As clearly seen in the inset of Figure 6, the time dependence of $C_L(t)/C_L(0)$ around $t \cong 0$ is approximated as $1 - (u_2/2)\ t^2 + O(t^4)$ or $\exp[-(u_2/2)\ t^2] + O(t^4)$ with $u_2 > 0$. [Note that $C_L(-t) = C_L(t)$ from eq 18.] On the basis of the stationary nature of the frequency modulations,[77] u_2 is related to the time scale of the frequency modulation as

$$u_2 = \left\langle \frac{1}{N}\sum_{m=1}^{N} \left(\frac{d}{dt}\delta\tilde{\nu}_m^{(L)}(t)\right)^2 \Big|_{t=0} \right\rangle \Big/ \left\langle \frac{1}{N}\sum_{m=1}^{N} (\delta\tilde{\nu}_m^{(L)}(0))^2 \right\rangle \tag{20}$$

From the fitting to the plot of $C_L(t)/C_L(0)$ in the first 6 fs, we obtain $u_2 = 2.65 \times 10^3\ ps^{-2}$ for neat liquid H_2O. The correlation time defined as the integral of $\exp[-(u_2/2)\ t^2]$ is calculated as $\tau_C = (\pi/2u_2)^{1/2} \cong 24.4$ fs, which is close to the experimental estimation of $\tau_C \cong 30$ fs.[78] Combining with the value of Δ_f ($\equiv [C_L(0)]^{1/2}$) $= 1.90 \times 10^2\ cm^{-1}$, we have $2\pi c\tau_C\Delta_f = 0.87$,[79] which is close to unity, indicating that the frequency modulation is (on the average) in the intermediate case.[25]

Because the vibrational frequencies are modulated by the electric field from the surrounding molecules according to the mechanism described by eq 13, with the interaction point being located on the hydrogen atom of each OH oscillator, and the electric field is considered to originate mainly from the oxygen atom (hydrogen-bond acceptor) of the hydrogen-bonded molecule, it is expected that the behavior of $C_L(t)$ is similar to that of the correlation function of hydrogen-bond lengths. To examine this point, the correlation function defined as

$$C_{HB}(t) = \left\langle \frac{1}{N}\sum_{m=1}^{N} \delta\left(\frac{1}{[r_m^{(O\cdots H)}(t)]^2}\right)\delta\left(\frac{1}{[r_m^{(O\cdots H)}(0)]^2}\right) \right\rangle \tag{21}$$

is calculated, where

$$\delta\left(\frac{1}{[r_m^{(O\cdots H)}(t)]^2}\right) = \frac{1}{[r_m^{(O\cdots H)}(t)]^2} - \left\langle \frac{1}{N}\sum_{m=1}^{N} \frac{1}{[r_m^{(O\cdots H)}]^2} \right\rangle \tag{22}$$

and $r_m^{(O\cdots H)}(t)$ is the distance between the hydrogen atom of the mth oscillator and its nearest oxygen atom (except the oxygen atom in the same molecule) at time t. To model the effect of electric field, the inverse square of the hydrogen-bond length rather than the length itself is taken in the definition of $C_{HB}(t)$. The result is shown with an orange line in Figure 6. It is seen that the behavior of $C_{HB}(t)/C_{HB}(0)$ is indeed quite similar to that of $C_L(t)/C_L(0)$. This result supports the suggestion made in a previous experimental study[38] that the measurement of the photon echo peak shift provides information on the dynamical properties of hydrogen bonds.

D. Time Evolution of the Extent of Delocalization of Vibrational Excitations. To examine the relation between the rapid decay of the TRIR anisotropy and the delocalization of vibrational excitations, the time evolution of the extent of delocalization of the initially localized vibrational excitations, denoted as $d(t)$, is calculated for the OH stretching mode of neat liquid H_2O. It is expressed as[23,24]

$$d(t) = \left\langle \frac{1}{N}\sum_{m=1}^{N} \left(\sum_{n=1}^{N} |z_{nm}(t)|^4\right)^{-1} \right\rangle \tag{23}$$

where $z_{nm}(t)$ is the transfer amplitude of the vibrational excitation from the mth to the nth oscillator, defined as

$$z_{nm}(t) = \left\langle n \left| \exp_+\left[-\frac{i}{\hbar}\int_0^t d\tau\ H^{1Q}(\tau)\right] \right| m \right\rangle \tag{24}$$

It is noted that eq 23 is valid as far as $\sum_{n=1}^{N}|z_{nm}(t)|^2$ is equal to unity. When the vibrational population relaxation is explicitly taken into account, the transfer amplitude $z_{nm}(t)$ should be normalized before evaluating eq 23. The result (calculated with $\zeta = 0.32\ e^2\ m_e^{-1/2}\ a_0\ E_h^{-1}$ at 298 K) is shown in Figure 7. It is seen that initially localized vibrational excitations become delocalized over ~3 oscillators in the first 0.1 ps and over ~20 oscillators in about 0.55 ps. The values of the same quantity calculated for the amide I mode of liquid *N*,*N*-dimethylformamide (DMF)[24] and the C=O stretching mode of liquid acetone[23] are also shown for comparison. The delocalization rate calcu-

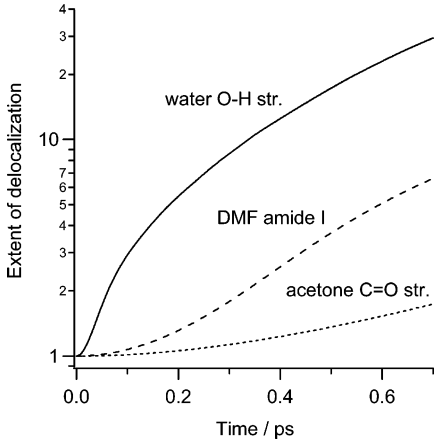

Figure 7. Time evolution of the extent of delocalization of the initially localized vibrational excitations $d(t)$ as defined by eq 23, calculated for the OH stretching mode of neat liquid H_2O with $|(\partial \boldsymbol{\mu}_m/\partial q_m)_0| = 0.6 \times 10^{-2}\ e\ m_e^{-1/2}$, $\zeta = 0.32\ e^2\ m_e^{-1/2}\ a_0\ E_h^{-1}$, and $k'_{mn} = 0$ (solid line). The plots for the amide I mode of liquid *N*,*N*-dimethylformamide (broken line, data from ref 24) and the C═O stretching mode of liquid acetone (dotted line, data from ref 23) are also shown.

lated for the OH stretching mode of neat liquid H_2O is much faster than that of the other two cases.

This faster delocalization rate is considered to be due to the larger magnitude of the intermolecular vibrational coupling. According to the TDC mechanism, as shown in eq 14, the magnitude of the intermolecular vibrational coupling is proportional to the square of the dipole derivative and the inverse cube of the intermolecular distance. The average magnitude of the dipole derivative of the OH stretching mode of neat liquid H_2O is calculated as $1.5911 \times 10^{-2}\ e\ m_e^{-1/2}$ (with $\zeta = 0.32\ e^2\ m_e^{-1/2}\ a_0\ E_h^{-1}$ at 298 K), which is nearly equal to that of the amide I mode of liquid DMF ($1.5407 \times 10^{-2}\ e\ m_e^{-1/2}$)[24] and is larger than that of the C═O stretching mode of liquid acetone ($1.0143 \times 10^{-2}\ e\ m_e^{-1/2}$).[23] The molecular volume of water (∼30 Å^3) is much smaller than that of the other two liquids (∼129 Å^3 for DMF and ∼122 Å^3 for acetone), indicating the shorter intermolecular distances in the former. Combining these two factors, the larger intermolecular vibrational coupling operating among the OH stretching oscillators in neat liquid H_2O is rationalized.

Comparing with the time constant of the decay of the TRIR anisotropy ($\tau = 0.10$ ps), it is recognized that the TRIR anisotropy decays in the time needed for the initially localized vibrational excitations to delocalize over a few oscillators. This result supports the suggestion obtained in a previous study[24] for the amide I mode of liquid DMF on the relation between the delocalization speed of vibrational excitations and the decay rate of the TRIR anisotropy.

5. Summary

In the present study, the polarized Raman spectra and the time dependence of the TRIR anisotropy have been calculated for the OH stretching mode of neat liquid H_2O by using the time-domain computational method developed in our previous study,[23] which takes into account the effects of both the diagonal frequency modulations (of individual oscillators) and the off-diagonal (intermolecular) vibrational coupling. The IR spectrum of neat liquid H_2O and the TRIR anisotropy of a liquid mixture of H_2O/HDO/D_2O have also been calculated. On the basis of the reasonable agreement between the observed[1,2,30−33] and calculated features of these optical signals, the intermolecular interactions and the dynamics that affect those spectroscopic features have been examined.

The conclusions obtained in this study may be summarized as follows. (1) The frequency separation between the first moments of the isotropic and anisotropic components of the polarized Raman spectrum (which is regarded as the NCE, shown in Figure 1) and the rapid decay of the TRIR anisotropy ($A(t)$, shown in Figure 5) of the OH stretching mode of neat liquid H_2O are mainly controlled by the resonant intermolecular vibrational coupling described by the TDC mechanism (eq 14). From the comparison of the behavior between $A(t)$ and the function $d(t)$ (defined by eq 23, shown in Figure 7), it is recognized that $A(t)$ decays in the time needed for the initially localized vibrational excitations to delocalize over a few oscillators, as suggested in our previous study[24] for the amide I mode of liquid DMF. (2) The intermolecular vibrational coupling of the OH stretching mode of neat liquid H_2O is stronger than those of the amide I mode of liquid DMF and the C═O stretching mode of liquid acetone. This is seen in the faster delocalization speed of the initially localized vibrational excitations (shown in Figure 7), and is rationalized by comparing the magnitudes of the dipole derivatives and the intermolecular distances. As a function of the number of neighboring oscillators (N_B), the magnitude of the coupling decreases as $-H_{mn}^{1Q} \sim N_B^{-1.29}$ and $|H_{mn}^{1Q}| \sim N_B^{-1.07}$ (shown in Figure 4), faster than the r^{-3} dependence arising from the denominator of H_{mn}^{1Q} (eq 14). Qualitatively, this behavior is not peculiar to liquid water or hydrogen-bonding liquids. (3) The intramolecular vibrational coupling is considered to be small for the OH stretching mode of H_2O in liquid water, as suggested in some previous studies.[64−66] A large value of this coupling leads to disagreement in the spectrum of the depolarization ratio ρ (shown in Figure 2) with the experiment,[32] and does not explain the time dependence of the TRIR anisotropy $A(t)$ (shown in Figure 5). (4) The enhancement of the dipole derivatives by the interactions with surrounding molecules, introduced by the parameter ζ, is an important factor in generating the spectral profiles of the OH stretching Raman bands, as suggested in some previous studies.[56,57] The effect of this factor is also seen in the behavior of $A(t)$ of a liquid mixture of H_2O/HDO/D_2O in the first 50 fs (shown in Figure 6), and the enhancement of the total intensity of the IR spectrum that occurs upon decreasing the temperature. (5) The vibrational frequencies of individual OH stretching oscillators are also modulated by the interactions with surrounding molecules. The time dependence of the correlation function $C_L(t)$ (defined by eq 18, shown in Figure 6) is in reasonable agreement with that obtained from the observed photon echo peak shift,[38,75] suggesting the validity of the mechanism of the frequency shift (eq 13), and is mainly explained by modulations of the hydrogen-bond lengths [$C_{HB}(t)$ defined by eq 21]. From the value of $2\pi c\tau_C\Delta_f = 0.87$, the speed of this modulation is considered to be (on the average) in the intermediate case. (6) The overall behavior of $A(t)$ of a liquid mixture of H_2O/HDO/D_2O, including the rapid decay in the first 25 fs, is mainly controlled by the librational motions of water molecules described by the correlation function $C_{R2}(t)$ defined by eq 17, as shown in Figure 6. However, the slightly faster decay of $A(t)$ as compared with that of $C_{R2}(t)$ in the region of $t \geq 0.2$ ps is considered to be due to the weak intermolecular vibrational coupling among the OH oscillators present even in the liquid mixture of H_2O/HDO/D_2O.

The results in the present paper have clearly shown how the spectroscopic features of the OH stretching mode of liquid water in the time and frequency domains are affected by the delocal-

ized nature of vibrational excitations and the modulations induced by liquid dynamics. It is expected that they will help to obtain deeper insight into the behavior of vibrational excitations in liquids.

Acknowledgment. This study was supported by a Grant-in-Aid for Scientific Research from the Ministry of Education, Culture, Sports, Science, and Technology, Japan and by a grant from the Morino Foundation for Molecular Science.

References and Notes

(1) Woutersen, S.; Bakker, H. J. *Nature (London)* **1999**, *402*, 507.
(2) Cowan, M. L.; Bruner, B. D.; Huse, N.; Dwyer, J. R.; Chugh, B.; Nibbering, E. T. J.; Elsaesser, T.; Miller, R. J. D. *Nature (London)* **2005**, *434*, 199.
(3) Torii, H. In *Novel Approaches to the Structure and Dynamics of Liquids: Experiments, Theories and Simulations*; Samios, J., Durov. V. A., Eds.; Kluwer: Dordrecht, The Netherlands, 2004; p 343.
(4) Torii, H. *Chem. Phys. Lett.* **2000**, *323*, 382.
(5) Fini, G.; Mirone, P.; Fortunato, B. *J. Chem. Soc., Faraday Trans. 2* **1973**, *69*, 1243.
(6) Perchard, C.; Perchard, J. P. *J. Raman Spectrosc.* **1975**, *3*, 277.
(7) Schindler, W.; Sharko, P. T.; Jonas, J. *J. Chem. Phys.* **1982**, *76*, 3493.
(8) Giorgini, M. G.; Fini, G.; Mirone, P. *J. Chem. Phys.* **1983**, *79*, 639.
(9) Zerda, T. W.; Thomas, H. D.; Bradley, M.; Jonas, J. *J. Chem. Phys.* **1987**, *86*, 3219.
(10) Sokolowska, A.; Kecki, Z. *J. Raman Spectrosc.* **1993**, *24*, 331.
(11) Mortensen, A.; Faurskov Nielsen, O.; Yarwood, J.; Shelley, V. *J. Phys. Chem.* **1994**, *98*, 5221.
(12) Musso, M.; Giorgini, M. G.; Döge, G.; Asenbaum, A. *Mol. Phys.* **1997**, *92*, 97.
(13) Bertie, J. E.; Michaelian, K. H. *J. Chem. Phys.* **1998**, *109*, 6764.
(14) Schweitzer-Stenner, R.; Sieler, G.; Mirkin, N. G.; Krimm, S. *J. Phys. Chem. A* **1998**, *102*, 118.
(15) Giorgini, M. G.; Musso, M.; Asenbaum, A.; Döge, G. *Mol. Phys.* **2000**, *98*, 783.
(16) Musso, M.; Torii, H.; Ottaviani, P.; Asenbaum, A.; Giorgini, M. G. *J. Phys. Chem. A* **2002**, *106*, 10152.
(17) Giorgini, M. G.; Musso, M.; Torii, H. *J. Phys. Chem. A* **2005**, *109*, 5846.
(18) Musso, M.; Giorgini, M. G.; Torii, H.; Dorka, R.; Schiel, D.; Asenbaum, A.; Keutel, D.; Oehme, K.-L. *J. Mol. Liq.* **2006**, *125*, 115.
(19) McHale, J. L. *J. Chem. Phys.* **1981**, *75*, 30.
(20) Logan, D. E. *Chem. Phys.* **1986**, *103*, 215.
(21) Torii, H.; Tasumi, M. *J. Chem. Phys.* **1993**, *99*, 8459.
(22) Torii, H. *J. Phys. Chem. A* **2002**, *106*, 3281.
(23) Torii, H.; Musso, M.; Giorgini, M. G. *J. Phys. Chem. A* **2005**, *109*, 7797.
(24) Torii, H. *J. Phys. Chem. A* **2006**, *110*, 4822.
(25) Kubo, R. *Adv. Chem. Phys.* **1969**, *15*, 101.
(26) Bell, R. J.; Dean, P. *Discuss. Faraday Soc.* **1970**, *50*, 55.
(27) Thouless, D. J. *Phys. Rep.* **1974**, *13*, 93.
(28) Weaire, D.; Williams, A. R. *J. Phys. C: Solid State Phys.* **1977**, *10*, 1239.
(29) Evensky, D. A.; Scalettar, R. T.; Wolynes, P. G. *J. Phys. Chem.* **1990**, *94*, 1149.
(30) Murphy, W. F.; Bernstein, H. J. *J. Phys. Chem.* **1972**, *76*, 1147.
(31) Scherer, J. R.; Go, M. K.; Kint, S. *J. Phys. Chem.* **1974**, *78*, 1304.
(32) Walrafen, G. E. *J. Chem. Phys.* **2005**, *122*, 174502.
(33) Brubach, J.-B.; Mermet, A.; Filabozzi, A.; Gerschel, A.; Roy, P. *J. Chem. Phys.* **2005**, *122*, 184509.
(34) Mukamel, S. *Principles of Nonlinear Optical Spectroscopy*, Oxford University Press: New York, 1995.
(35) An "overtone" state stands for a state with two quanta on a single oscillator, which is distinguished from a "combination" state with one quantum each on two oscillators.
(36) Ham, S.; Kim, J. H.; Lee, H.; Cho, M. *J. Chem. Phys.* **2003**, *118*, 3491.
(37) Bouř, P.; Keiderling, T. A. *J. Chem. Phys.* **2003**, *119*, 11253.
(38) Fecko, C. J.; Eaves, J. D.; Loparo, J. J.; Tokmakoff, A.; Geissler, P. L. *Science* **2003**, *301*, 1698.
(39) Hayashi, T.; Hamaguchi, H. *Chem. Phys. Lett.* **2000**, *326*, 115.
(40) Corcelli, S. A.; Lawrence, C. P.; Skinner, J. L. *J. Chem. Phys.* **2004**, *120*, 8107.
(41) Schmidt, J. R.; Corcelli, S. A.; Skinner, J. L. *J. Chem. Phys.* **2004**, *121*, 8887.
(42) Torii, H. *J. Phys. Chem. A* **2002**, *106*, 1167.
(43) Torii, H. *J. Phys. Chem. A* **2004**, *108*, 7272.
(44) Hayashi, T.; Jansen, T. l. C.; Zhuang, W.; Mukamel, S. *J. Phys. Chem. A* **2005**, *109*, 64.
(45) Hush, N. S.; Reimers, J. R. *J. Phys. Chem.* **1995**, *99*, 15798.
(46) Andrews, S. S.; Boxer, S. G. *J. Phys. Chem. A* **2002**, *106*, 469.
(47) Torii, H. *J. Chem. Phys.* **2003**, *119*, 2192.
(48) Haas, C.; Hornig, D. F. *J. Chem. Phys.* **1960**, *32*, 1763.
(49) Belch, A. C.; Rice, S. A. *J. Chem. Phys.* **1983**, *78*, 4817.
(50) Rice, S. A.; Bergren, M. S.; Belch, A. C.; Nielsen, G. *J. Phys. Chem.* **1983**, *87*, 4295.
(51) Wiafe-Akenten, J.; Bansil, R. *J. Chem. Phys.* **1983**, *78*, 7132.
(52) Buch, V. *J. Phys. Chem. B* **2005**, *109*, 17771.
(53) Krimm, S.; Abe, Y. *Proc. Natl. Acad. Sci. U.S.A.* **1972**, *69*, 2788.
(54) Torii, H.; Tasumi, M. *J. Chem. Phys.* **1992**, *96*, 3379.
(55) This treatment is similar to the one adopted in our previous study (ref 16), where the dipole derivative of the OH stretching mode of methanol was assumed to be a function of the hydrogen-bond length.
(56) Corcelli, S. A.; Skinner, J. L. *J. Phys. Chem. A* **2005**, *109*, 6154.
(57) Schmidt, J. R.; Corcelli, S. A.; Skinner, J. L. *J. Chem. Phys.* **2005**, *123*, 044513.
(58) Shimanouchi, T. *Tables of Molecular Vibrational Frequencies Consolidated Volume I*; National Bureau of Standards: Washington, DC, 1972.
(59) Frisch, M. J.; Trucks, G. W.; Schlegel, H. B.; Scuseria, G. E.; Robb, M. A.; Cheeseman, J. R.; Montgomery, J. A., Jr.; Vreven, T.; Kudin, K. N.; Burant, J. C.; Millam, J. M.; Iyengar, S. S.; Tomasi, J.; Barone, V.; Mennucci, B.; Cossi, M.; Scalmani, G.; Rega, N.; Petersson, G. A.; Nakatsuji, H.; Hada, M.; Ehara, M.; Toyota, K.; Fukuda, R.; Hasegawa, J.; Ishida, M.; Nakajima, T.; Honda, Y.; Kitao, O.; Nakai, H.; Klene, M.; Li, X.; Knox, J. E.; Hratchian, H. P.; Cross, J. B.; Adamo, C.; Jaramillo, J.; Gomperts, R.; Stratmann, R. E.; Yazyev, O.; Austin, A. J.; Cammi, R.; Pomelli, C.; Ochterski, J. W.; Ayala, P. Y.; Morokuma, K.; Voth, G. A.; Salvador, P.; Dannenberg, J. J.; Zakrzewski, V. G.; Dapprich, S.; Daniels, A. D.; Strain, M. C.; Farkas, O.; Malick, D. K.; Rabuck, A. D.; Raghavachari, K.; Foresman, J. B.; Ortiz, J. V.; Cui, Q.; Baboul, A. G.; Clifford, S.; Cioslowski, J.; Stefanov, B. B.; Liu, G.; Liashenko, A.; Piskorz, P.; Komaromi, I.; Martin, R. L.; Fox, D. J.; Keith, T.; Al-Laham, M. A.; Peng, C. Y.; Nanayakkara, A.; Challacombe, M.; Gill, P. M. W.; Johnson, B.; Chen, W.; Wong, M. W.; Gonzalez, C.; Pople, J. A. *Gaussian 03, Revision C.02*, Gaussian, Inc.: Wallingford CT, 2004.
(60) To extract the OH stretching motion of a single hydrogen-bonded OH bond from the normal modes, we used the average partial vector method described in ref 43.
(61) Jorgensen, W. L.; Chandrasekhar, J.; Madura, J. D.; Impey, R. W.; Klein, M. L. *J. Chem. Phys.* **1983**, *79*, 926.
(62) The density at 263.15 K was estimated by extrapolation.
(63) Mills, R. *J. Phys. Chem.* **1973**, *77*, 685.
(64) Bertie, J. E.; Bates, F. E. *J. Chem. Phys.* **1977**, *67*, 1511.
(65) Rice, S. A.; Sceats, M. G. *J. Phys. Chem.* **1981**, *85*, 1108.
(66) Green, J. L.; Lacey, A. R.; Sceats, M. G. *J. Phys. Chem.* **1986**, *90*, 3958.
(67) Mahoney, M. W.; Jorgensen, W. L. *J. Chem. Phys.* **2000**, *112*, 8910.
(68) Okumura, K.; Tokmakoff, A.; Tanimura, Y. *J. Chem. Phys.* **1999**, *111*, 492.
(69) Loparo, J. J.; Fecko, C. J.; Eaves, J. D.; Roberts, S. T.; Tokmakoff, A. *Phys. Rev. B* **2004**, *70*, 180201.
(70) Fecko, C. J.; Loparo, J. J.; Roberts, S. T.; Tokmakoff, A. *J. Chem. Phys.* **2005**, *122*, 054506.
(71) Rezus, Y. L. A.; Bakker, H. J. *J. Chem. Phys.* **2005**, *123*, 114502.
(72) Rahman, A.; Stillinger, F. H. *J. Chem. Phys.* **1971**, *55*, 3336.
(73) Walrafen, G. E. *J. Chem. Phys.* **1964**, *40*, 3249.
(74) Piryatinski, A.; Lawrence, C. P.; Skinner, J. L. *J. Chem. Phys.* **2003**, *118*, 9672.
(75) Stenger, J.; Madsen, D.; Hamm, P.; Nibbering, E. T. J.; Elsaesser, T. *J. Phys. Chem. A* **2002**, *106*, 2341.
(76) Asbury, J. B.; Steinel, T.; Kwak, K.; Corcelli, S. A.; Lawrence, C. P.; Skinner, J. L.; Fayer, M. D. *J. Chem. Phys.* **2004**, *121*, 12431.
(77) Kubo, R.; Toda, M.; Hashitsume, N. *Statistical Physics II, Non-equilibrium Statistical Mechanics*; Springer: Berlin, 1985.
(78) Stenger, J.; Madsen, D.; Hamm, P.; Nibbering, E. T. J.; Elsaesser, T. *Phys. Rev. Lett.* **2001**, *87*, 027401.
(79) For the liquid mixture of $H_2O/HDO/D_2O$, we obtain $u_2 = 2.22 \times 10^3$ ps^{-2}, $\tau_C = 26.6$ fs, and $\Delta_f = 1.89 \times 10^2$ cm^{-1}, leading to $2\pi c\tau_C\Delta_f = 0.95$.